Impaired defense mechanism against inflammation, hyperalgesia, and airway hyperreactivity in somatostatin 4 receptor gene-deleted mice

Zsuzsanna Helyes[a], Erika Pintér[a], Katalin Sándor[a], Krisztián Elekes[b], Ágnes Bánvölgyi[a], Dániel Keszthelyi[a], Éva Szőke[a], Dániel M. Tóth[c], Zoltán Sándor[c], László Kereskai[d], Gábor Pozsgai[a], Jeremy P. Allen[e], Piers C. Emson[e], Adrienn Markovics[a], and János Szolcsányi[a,1]

[a]Department of Pharmacology and Pharmacotherapy, [b]Institute of Pharmacognosy, [c]Analgesic Research Laboratory of Gedon Richter Plc., and [d]Department of Pathology, Faculty of Medicine, University of Pécs, H-7624 Pécs, Hungary; and [e]Laboratory of Molecular Neuroscience, The Babraham Institute, Babraham Research Campus, Babraham, Cambridge CB22 3AT, United Kingdom

Edited by David Julius, University of California, San Francisco, CA, and approved June 3, 2009 (received for review January 21, 2009)

We have shown that somatostatin released from activated capsaicin-sensitive nociceptive nerve endings during inflammatory processes elicits systemic anti-inflammatory and analgesic effects. With the help of somatostatin receptor subtype 4 gene–deleted mice ($sst_4^{-/-}$), we provide here several lines of evidence that this receptor has a protective role in a variety of inflammatory disease models; several symptoms are more severe in the sst_4 knockout animals than in their wild-type counterparts. Acute carrageenan-induced paw edema and mechanical hyperalgesia, inflammatory pain in the early phase of adjuvant-evoked chronic arthritis, and oxazolone-induced delayed-type hypersensitivity reaction in the skin are much greater in mice lacking the sst_4 receptor. Airway inflammation and consequent bronchial hyperreactivity elicited by intranasal lipopolysaccharide administration are also markedly enhanced in sst_4 knockouts, including increased perivascular/peribronchial edema, neutrophil/macrophage infiltration, mucus-producing goblet cell hyperplasia, myeloperoxidase activity, and IL-1β, TNF-α, and IFN-γ expression in the inflamed lung. It is concluded that during these inflammatory conditions the released somatostatin has pronounced counterregulatory effects through sst_4 receptor activation. Thus, this receptor is a promising novel target for developing anti-inflammatory, analgesic, and anti-asthmatic drugs.

allergic contact dermatitis | arthritis | capsaicin-sensitive afferents | endotoxin-induced pneumonitis | inflammatory cytokines

We and others have previously reported that somatostatin is released from capsaicin-sensitive nociceptive nerve endings in response to chemical and antidromic electrical stimulation of these fibers (1). Several lines of further functional evidence have also indicated that somatostatin derived from these nerves reaches the circulation and elicits systemic anti-inflammatory and antinociceptive effects (1–4). Calcium influx into the nerve terminals elicits the release of both proinflammatory (substance P and calcitonin gene-related peptide) and anti-inflammatory neuropeptides without the involvement of voltage-gated channels (3). Nevertheless, these peptides are only partially colocalized in most primary afferents (5, 6), and whereas substance P− and calcitonin gene-related peptide–immunoreactive fibers are present in the superficial areas, somatostatin-containing ones are only seen in deeper layers (7). Therefore, it is likely that when noxious stimuli reach deeper tissues—besides the local inflammatory response—the released somatostatin elicits systemic anti-inflammatory actions too. This was shown by our group in adjuvant-induced chronic arthritis (8), as well as in endotoxin-induced airway inflammation and polyneuropathic conditions (9).

Somatostatin is widely distributed throughout the body in 14 aa- and 28 aa-containing forms (7, 10, 11). Besides its localization in sensory neurons (for review see refs. 5, 6, and 12), it is also produced by neuroendocrine cells (gastrointestinal intrinsic neurons, pancreas, and thyroid C cells), as well as inflammatory and immune cells (lymphocytes, macrophages, thymic epithelial cells, activated synovial cells, and fibroblasts) (4, 11, 13). Somatostatin exerts a wide range of effects in the central nervous system and in the periphery (for review see ref. 11), which are mediated via 5 different G_i protein–associated somatostatin receptor subtypes (sst_1–sst_5). They can be divided into 2 main groups on the basis of sequence similarities and binding of synthetic somatostatin analogues: the somatostatin release-inhibiting factor 1 ($SRIF_1$) group comprises sst_2, sst_3, and sst_5 receptors, and the $SRIF_2$ group contains sst_1 and sst_4 receptors (14). Each receptor is coupled to the inhibition of adenylate cyclase and the cAMP/protein kinase A via pertussis toxin sensitive GTP binding proteins (4, 10, 11). These inhibitory actions of somatostatin might provide the link between sst_4 receptor activation and modulation of other receptors and/or ion channels (e.g., opioid or cannabinoid receptors). Furthermore, sst receptor activation opens various K^+ channels and inhibits voltage-gated Ca^{2+} channels, which results in inhibition of both spike generation and release of neurotransmitters (for review see ref. 4). Several data indicate that receptors in the $SRIF_1$ group mediate the endocrine and antiproliferative effects, whereas the $SRIF_2$ group, predominantly the sst_4 receptor, is responsible for the anti-inflammatory and antinociceptive actions (3, 15, 16).

On the basis of these data we have raised the possibility that this receptor may be a promising target for anti-inflammatory and analgesic agents with a novel mechanism of action. Because specific sst_4 receptor antagonists are not available, generation of sst_4 receptor gene–deficient mice is a useful tool to elucidate the role of these receptors in inflammatory processes.

The present article describes the generation of sst_4 receptor knockout mice and investigates the involvement of the sst_4 receptor in different acute and chronic inflammatory disease models.

Results

Generation of sst_4 Receptor Gene-Deficient Mice. The generation of the sst_4^{lacZ} allele was essentially carried out as described for sst_2^{lacZ} animals (17). In the sst_4 targeting cassette the Ura3/Neo selection cassette was flanked by LoxP sites to enable its removal

Author contributions: Z.H., E.P., and J.S. designed research; Z.H., K.S., K.E., A.B., D.K., E.S., Z.S., L.K., G.P., and A.M. performed research; J.P.A. and P.C.E. contributed new reagents/analytic tools; K.S., K.E., and D.M.T. analyzed data; and Z.H., E.P., and J.S. wrote the paper.

The authors declare no conflict of interest.

This article is a PNAS Direct Submission.

[1]To whom correspondence should be addressed. E-mail: janos.szolcsanyi@aok.pte.hu.

This article contains supporting information online at www.pnas.org/cgi/content/full/0900681106/DCSupplemental.

www.pnas.org/cgi/doi/10.1073/pnas.0900681106

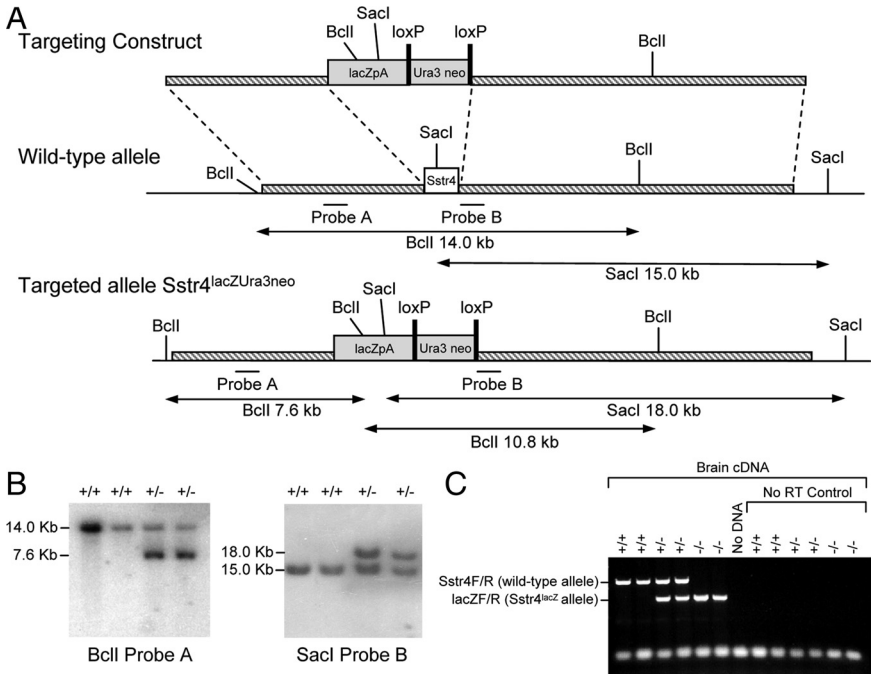

Fig. 1. Generation of sst_4 receptor gene–deficient mice. (*A*) Targeting strategy used for gene disruption of the mouse sst_4 genomic locus. The 1155-bp coding sequence of sst_4 resides on a single exon (white box). A replacement vector was designed to delete the entire sst_4 coding sequence and replace it with a cassette comprising a nuclear localized lacZ reporter gene (lacZpA) and loxP-flanked selectable markers uracil3 (Ura3) and neomycin resistance (neo) (shaded boxes). The initiation codon of lacZ is inserted, in frame, into the initiation codon of sst_4. (*B*) Southern blot analysis of genomic DNA prepared from tail biopsies of an sst_4 mutant pedigree shows correct targeting. DNAs were digested with BclI and hybridized with probe A or digested with SacI and hybridized with probe B ($sst_4^{+/+}$: +/+; $sst_4^{+/lacZUra3neo}$: +/-). (*C*) RT-PCR analysis of sst_4 and lacZ transcription. RT-PCR from total brain RNA using multiplexed sst_4 and lacZ primer sets demonstrates the presence of sst_4 mRNA in $sst_4^{+/+}$ and $sst_4^{+/lacZ}$ but an absence in $sst_4^{lacZ/lacZ}$ mice. Conversely, lacZ mRNA is detected in $sst_4^{+/lacZ}$ and $sst_4^{lacZ/lacZ}$ but is absent from $sst_4^{+/+}$ animals ($sst_4^{+/+}$: +/+; $sst_4^{+/lacZ}$: +/-; $sst_4^{lacZ/lacZ}$: -/-). No amplification was observed when RT-PCR was performed in the absence of reverse transcriptase (No RT Control) or when PCR was performed in the absence of cDNA template (No DNA).

after targeting (Fig. 1*A*). The vector was transfected into 129/Ola-derived E-14 embryonic stem cells by electroporation, followed by G418 selection. Correctly targeted clones carrying a $sst_4^{+/lacZUra3neo}$ allele were identified by Southern blot analysis using probes A and B and microinjected into C57BL/6 blastocysts to produce chimeric mice. Chimeric males were mated to C57BL/6 to generate heterozygous animals. Heterozygous intercross of $sst_4^{lacZ/Ura3/Neo}$ mice produced viable and fertile litters without obvious abnormalities at the expected Mendelian ratio. The genotype was determined by PCR and Southern blot analysis (Fig. 1*B*). Heterozygotes were then mated with *Cre-deletor* mice (18) that express Cre recombinase in germ cells. Deletion of the *loxP*-flanked selection cassette in F_1 animals to create the allele sst_4^{lacZ} was verified by Southern blot using probe B. The sst_4^{lacZ} allele was then backcrossed to C57BL/6 mice for a further 10 generations using males and females $sst_4^{+/lacZ}$ alternately. Homozygous $sst_4^{lacz/lacZ}$ and WT ($sst_4^{+/+}$) littermates were generated by intercrossing $sst_4^{+/lacZ}$ mice from the 10th generations of backcross mice. No sst_4 mRNA was detectable in the sst_4^{lacZ} mice, whereas lacZ was expressed (Fig. 1*C*). Animals were produced in accordance with United Kingdom Home Office guidelines and licensed under the Animals (Scientific Procedures) Act of 1986.

Increased Carrageenan-Induced Acute Mechanical Hyperalgesia and Paw Edema in $sst_4^{-/-}$ Mice. The control paw volumes ($sst_4^{+/+}$: 0.67 ± 0.02 cm^3; $sst_4^{-/-}$: 0.68 ± 0.02 cm^3) and the mechanonociceptive thresholds ($sst_4^{+/+}$: 8.3 ± 0.16 g; $sst_4^{-/-}$: 8.0 ± 0.14 g) of the 2 groups did not differ significantly. Carrageenan administration caused inflammation of the treated paw with a marked swelling, redness, and decrease of the mechanonociceptive threshold. Six hours after the injection both edema and the drop of the nociceptive threshold were significantly greater in the knockout group. The results of WT and sst_4, receptor-deficient littermates produced from heterozygote mice were essentially the same as data obtained in $sst_4^{+/+}$ and $sst_4^{-/-}$ mice bred as separate lines. Pretreatment with the selective peptidomimetic sst_4 receptor agonist J-2156 (100 μg/kg, i.p.) (19–21) 10 min before carrageenan significantly inhibited mechanical hyperalgesia in WT mice but not in the knockouts. Surprisingly, J-2156 did not inhibit paw swelling in either group (Fig. 2 *A* and *B*).

Adjuvant-Induced Chronic Paw Inflammation, Mechanical Hyperalgesia, and Impaired Spontaneous Weight Bearing in $sst_4^{-/-}$ Mice. Inflammatory mechanical hyperalgesia was greater in $sst_4^{-/-}$ mice than in their WT counterparts throughout the whole 21-day experimental period, but the difference was more pronounced and shown to be significant up to the 13th day of the study. Similarly, until this time significantly less weight was distributed on the treated hindlimb in the $sst_4^{-/-}$ than in the $sst_4^{+/+}$ group, but no difference could be observed later. Edema did not differ significantly in the 2 groups: paw swelling was between 80% and 100% throughout the whole period in both $sst_4^{+/+}$ and $sst_4^{-/-}$ mice.

Greater Endotoxin-Evoked Inflammatory Changes in the Lung and Enhanced Airway Responsiveness in $sst_4^{-/-}$ Mice. On the histologic slides marked peribronchial/perivascular edema, granulocyte accumulation, mononuclear cell infiltration, and hyperplasia of mucus-producing goblet cells were seen in response to LPS administration in both groups. In $sst_4^{-/-}$ mice the extent of the edema was greater, and the destruction of the alveolar spaces by the large number of infiltrating leukocytes and the hyperplasia of goblet cells were much more pronounced. The detailed scores

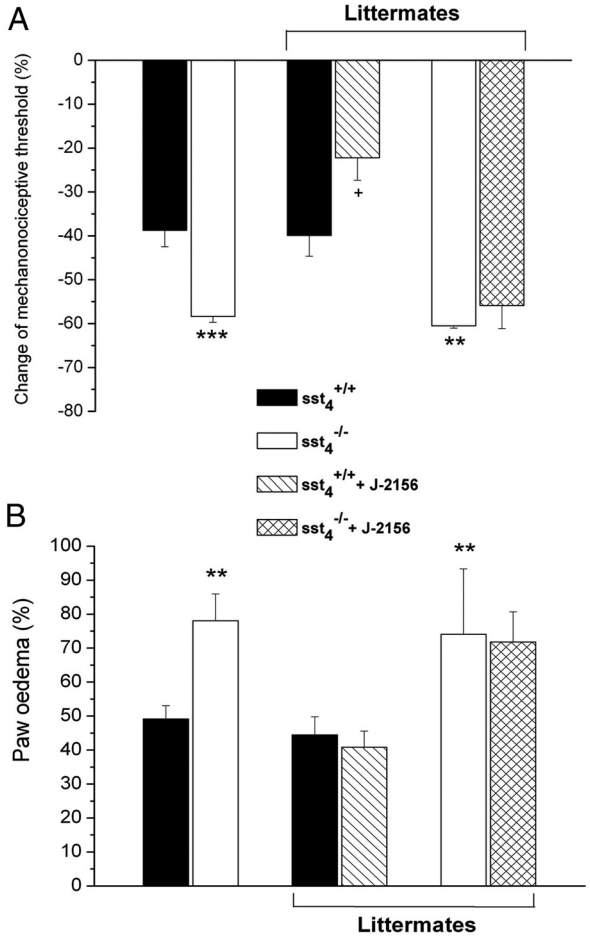

Fig. 2. (*A*) Decrease of the mechanonociceptive thresholds and (*B*) increase of the paw volume 6 h after intraplantar carrageenan (50 μL, 3%) injection in $sst_4^{+/+}$ and $sst_4^{-/-}$ mice. Percentage changes are calculated by comparing the data with the initial self-control values. Results obtained in $sst_4^{+/+}$ and $sst_4^{-/-}$ mice bred as separate lines, as well as littermate WT and knockouts, are indicated. The effect of the selective sst_4 receptor agonist J-2156 (100 μg/kg i.p.) is also shown in both group (means ± SEM of $n = 6–8$ experiments; $^*P < 0.05$, $^{**}P < 0.01$ vs the $sst_4^{+/+}$, group, $^+P < 0.05$ vs solvent treated $sst_4^{+/+}$ mice determined by one-way ANOVA followed by Bonferroni's modified *t* test).

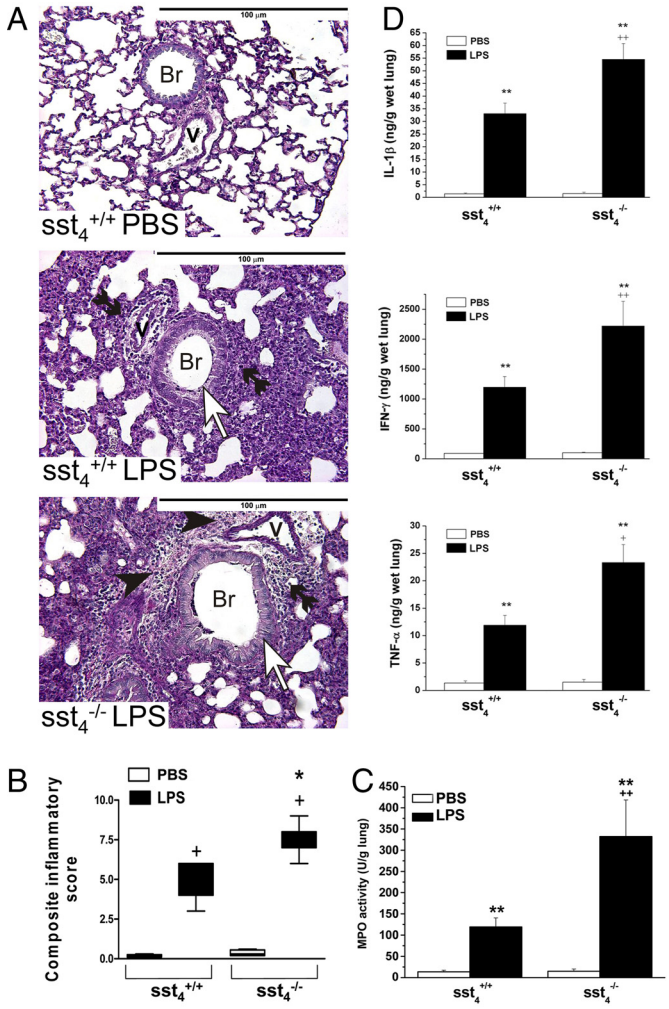

Fig. 3. Histopathologic examination, MPO activity, and inflammatory cytokine concentrations of the lung in LPS-induced inflammation. (*A*) Representative histopathologic pictures of the lung samples of $sst_4^{+/+}$ and $sst_4^{-/-}$ mice (periodic acid-Schiff staining; ×200; Br, bronchioles; V, vessels; open arrows indicate goblet cells, black arrowheads indicate edema formation, and double black arrowheads indicate granulocyte accumulation). (*B*) Semiquantitative evaluation and scoring of the lung on the basis of perivascular edema, perivascular/peribronchial granulocyte accumulation, goblet cell hyperplasia, and alveolar mononuclear cell infiltration. Columns represent medians with upper and lower quartiles of $n = 8–10$ mice; $^+P < 0.01$ LPS-treated inflamed vs. respective PBS-treated noninflamed mice; $^*P < 0.05$ LPS-treated $sst_4^{-/-}$ vs. LPS-treated $sst_4^{+/+}$ group (Kruskal-Wallis test plus Dunn's posttest). (*C*) MPO activity, as a quantitative indicator of the number of accumulated granulocytes, and (*D*) concentrations IL-1β, IFN-γ, and TNF-α determined from homogenized lung samples. Columns show means ± SEM of $n = 8–10$ mice; $^{**}P < 0.01$ vs. the respective noninflamed mice; $^{++}P < 0.01$ vs. the $sst_4^{+/+}$ group (one-way ANOVA plus Bonferroni's *t* test).

are shown in the supporting information *(SI) Text*; the representative light micrographs and composite values are presented in Fig. 3 *A* and *B*. In agreement with the histologic pictures, myeloperoxidase (MPO) activity increased in response to LPS instillation in both groups. This quantitative biochemical marker of accumulated granulocytes in the inflamed tissue was significantly (approximately 3-fold) greater in the $sst_4^{-/-}$ than in the $sst_4^{+/+}$ mice (Fig. 3*C*). Furthermore, LPS induced a 12–30-fold increase of IL-1β, IFN-γ, and TNF-α concentrations in the lung of WT mice, which was almost double in the sst_4 gene–deleted group (Fig. 3*D*).

Flow cytometric analysis of the bronchoalveolar lavage fluid (BALF) samples showed a remarkable accumulation of macrophages and lymphocytes in response to LPS in both groups, and the number of these cells was significantly greater in $sst_4^{-/-}$ mice (Fig. 4*C*). Significant increase of neutrophils occurred only in sst_4 knockouts, which is in agreement with the predominantly peribronchiolar/perivascular infiltration of these cells seen on the histologic slides. Similarly to the lung homogenates, the concentration of all of the 3 measured inflammatory cytokines markedly increased in the BALF of LPS-treated mice compared with noninflamed samples. Deletion of the sst_4 receptor significantly enhanced IFN-γ and TNF-α levels, but not IL-1β in the washing fluid (Fig. S1).

Both baseline enhanced pause (Penh) and lung resistance (RL) significantly increased after intranasal LPS instillation compared with PBS-treated, noninflamed control values, with no difference between the 2 mouse groups (*SI Text*). Carbachol inhalation evoked a concentration-dependent bronchoconstriction shown by both the Penh and RL curves. There was no significant difference between the carbachol-evoked responses of PBS-treated $sst_4^{+/+}$ and $sst_4^{-/-}$ animals. Responses demonstrated as percentage increase of Penh and RL above baseline were markedly enhanced in the LPS-treated groups compared

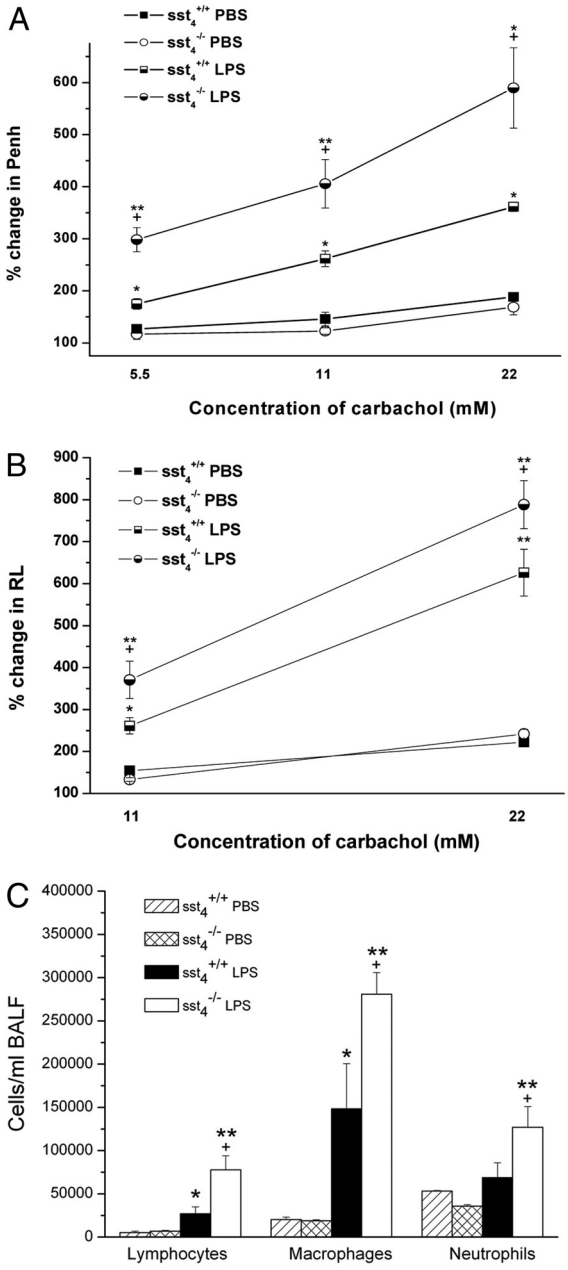

Fig. 4. Carbachol-evoked bronchoconstriction and inflammatory airway hyperreactivity in $sst_4^{+/+}$ and $sst_4^{-/-}$ mice. The panels demonstrate the percentage increases of (*A*) Penh and (*B*) RL above baseline [(mean values in response to the respective carbachol concentration- baseline values)/baseline values × 100] calculated in each 15-min period after respective carbachol stimulations. (*C*) Inflammatory cells accumulated in the BALF 24 h after intranasal endotoxin administration in $sst_4^{+/+}$ and $sst_4^{-/-}$ littermate mice. Data show means ± SEM of $n = 6$ mice per group; $^*P < 0.05$, $^{**}P < 0.01$ vs. the respective PBS-treated mice; $^+P < 0.05$, vs. the $sst_4^{+/+}$ group (one-way ANOVA plus Bonferroni's modified *t* test).

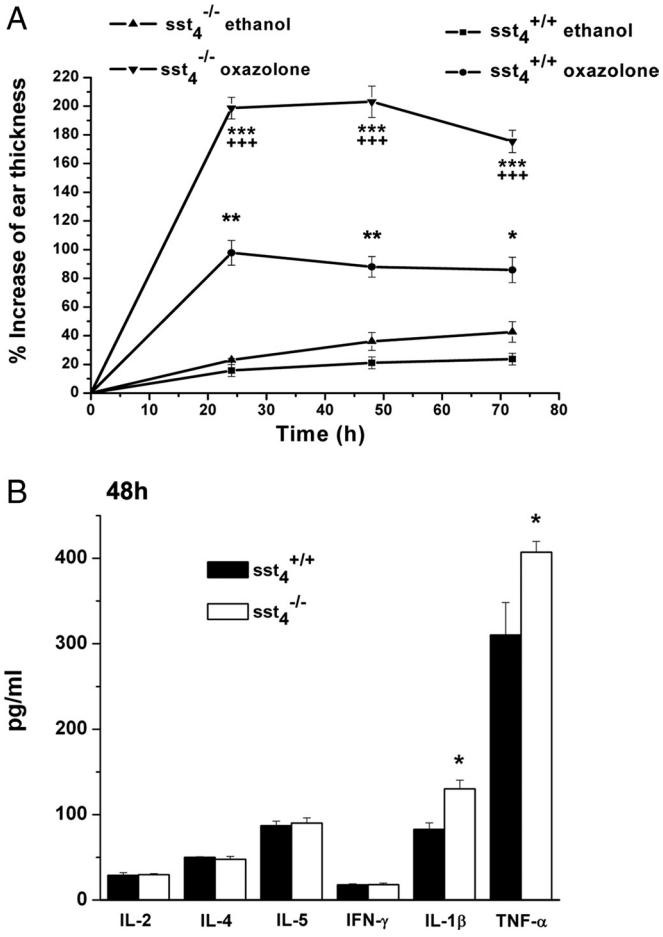

Fig. 5. Oxazolone-induced (*A*) swelling and (*B*) inflammatory cytokine concentrations of the ear of $sst_4^{+/+}$ and $sst_4^{-/-}$ mice. Edema data points represent means ± SEM percentage increase of ear diameter compared with the initial values of $n = 8$–10 experiments. $^*P < 0.05$, $^{**}P < 0.01$, $^{***}P < 0.001$ vs. respective ethanol-treated ears; $^{+++}P < 0.001$ vs. oxazolone-treated $sst_4^{+/+}$ mice. Columns showing cytokine concentrations in the ear homogenates 48 h after oxazolone application are means ± SEM of $n = 6$–8 per group. $^*P < 0.05$ vs. $sst_4^{+/+}$ (one-way ANOVA followed by Bonferroni's modified *t* test).

with the respective noninflamed controls, showing the development of inflammatory bronchial hyperresponsiveness. The maximal values were higher, the duration of bronchoconstriction was longer, and therefore the percentage increase of the responses above baseline was greater in mice lacking the sst_4 receptor (original records in Fig. S2). Comparison of the Penh responses determined in unrestrained mice and RL values measured in anesthetized and mechanically ventilated animals provided very similar results. This supports our previously published conclusions (9, 21) that although the validity of Penh in asthma models can be questioned, this is a reliable parameter to determine airway reactivity in the endotoxin-induced subacute airway inflammation model (Fig. 4 *A* and *B*).

More Severe Oxazolone-Induced Allergic Contact Dermatitis in $sst_4^{-/-}$ Mice. In WT mice, oxazolone induced an approximately 80–100% increase of ear thickness 24–48 h after its topical application. In knockout animals the edema was approximately double, 180–200% (Fig. 5*A*). Histologic analysis also showed greater swelling and even more intensive accumulation of inflammatory cells in the oxazolone-treated ears of $sst_4^{-/-}$ mice compared with their $sst_4^{+/+}$ controls (Fig. S3). Slightly raised levels of IL-4 and IL-5 cytokines and a remarkable elevation of IL-1β were detected in the ear samples 24 h after oxazolone smearing, but there was no difference between the 2 groups. At 48 h TNFα and IL-1β concentrations were higher in $sst_4^{-/-}$ mice than in WT animals (Fig. 5*B*).

Discussion

The present article describes the generation and the first in vivo data on sst_4 receptor knockout mice and provides several lines

PHYSIOLOGY

of evidence for the counterregulatory role of this receptor during inflammatory and nociceptive processes. Because sst_4-selective antagonists are not available, experiments with these genetically manipulated mice are particularly important to elucidate the role of sst_4 receptors in physiologic and pathophysiologic conditions. The inhibitory actions of sensory nerve–derived somatostatin in these well-established experimental models of inflammation have been previously shown (1, 8, 9, 22–24). This unique, systemic efferent protective function of these afferents was strongly supported in disease models such as adjuvant-induced chronic arthritis (8), endotoxin-evoked lung inflammation (9), oxazolone-induced allergic contact dermatitis (23), and bleomycin-evoked scleroderma (25). Direct evidence for the involvement of somatostatin of neural origin in the observed anti-inflammatory and analgesic actions was also provided (1–3, 8, 9). Results obtained with synthetic somatostatin receptor agonists suggested that these inhibitory effects were mediated by receptors of the $SRIF_2$ family (sst_4/sst_1) (8, 11, 15, 16, 19–21, 25). However, because of the lack of sst_4-selective antagonists, the precise receptor mechanisms of the somatostatin-mediated "sensocrine" inhibitory actions on inflammation and nociception have remained to be elucidated until the generation of sst_4 receptor gene–deficient mice.

Exogenous administration of somatostatin diminishes neurogenic vasodilatation, plasma protein extravasation, and the release of substance P from nerve endings (2). Inhibition of proliferation, infiltration, chemotaxis, and phagocytosis, as well as the release of reactive oxygen radicals and cytokines of inflammatory cells, are also well-documented effects of somatostatin (13, 16, 26–33). Sst_4 immunoreactivity was shown on vascular endothelial and smooth muscle cells (34), and its activation exerted protective effects (35). Sst_4 receptors are also present on peripheral blood monocytes, lymphocytes, fibroblasts, and endothelial cells (36, 37). In experimental rat arthritis predominantly sst_3 and sst_4 are expressed on immune cells, and in agreement with our earlier data, others also found that octreotide did not exert immunomodulatory actions in this model (11). The presence and inflammation-induced upregulation of sst_4 were observed in the human kidney and on capsaicin-sensitive afferents (15, 19). Opioid and cannabinoid receptors on nerves and inflammatory cells also linked to G_i proteins (38, 39) have been described as being involved in somatostatin signaling, which raises the possibility that knocking out the sst_4 receptor gene might also influence their function in inflammatory and nociceptive processes.

On the basis of the present results we suggest that somatostatin released during different inflammatory processes exerts a potent endogenous protective mechanism against edema formation and pathomorphologic and immunologic changes, as well as inflammatory pain and airway hyperresponsiveness. The edema-reducing effect of sst_4 receptor activation, however, was observed in the carrageenan-evoked acute inflammation and the allergic contact dermatitis models but not in adjuvant-induced chronic paw swelling. Although the increase of somatostatin-like immunoreactivity in the plasma was described earlier in the same complete Freund's adjuvant (CFA) model of rats (8), its sst_4 receptor–mediated inhibitory action on swelling is likely to be overridden by other immune cell–derived mediators, such as bradykinin, prostaglandins, histamine, serotonin, or leukotrienes. This seems to be the explanation for the disappearance of the antihyperalgesic and analgesic roles of sst_4 receptors after the 13th day of the experiment, by which time macrophages and lymphocytes have accumulated in the inflamed area (8).

Our previous data revealed that synthetic sst_4 receptor agonists—the heptapeptide TT-232 and the peptidomimetic J-2156—significantly attenuated several inflammatory processes with neurogenic and nonneurogenic mechanisms, such as mustard oil-, dextran-, carrageenan-, or bradykinin-induced acute plasma protein extravasation (15, 16, 19), adjuvant-induced chronic arthritis and hyperalgesia (8, 20), and endotoxin-induced acute and ovalbumin-evoked chronic lung inflammation and hyperresponsiveness (21). In most models the extent of the inhibition achieved by these agonists was similar to the difference found between the $sst_4^{+/+}$ and $sst_4^{-/-}$ groups. In the present experiment J-2156 inhibited carrageenan-evoked mechanical hyperalgesia, but in mice unlike in rats it did not alter paw swelling.

In conclusion, with the help of genetically manipulated mice we describe evidence for a previously uncharacterized counterregulatory mechanism mediated by sst_4 receptors during inflammatory and nociceptive processes. On the basis of these results, the sst_4 receptors localized on vascular endothelial, smooth muscle, inflammatory, and immune cells, as well as synoviocytes, may serve as promising new targets for the development of broad-spectrum anti-inflammatory and analgesic drugs.

Methods

Animals. Heterozygous mice ($sst_4^{+/-}$) were paired in the Laboratory Animal Center of Pécs University, and the genotype of their offsprings was determined by PCR. Sst_4 receptor gene–deficient ($sst_4^{-/-}$) and WT mice ($sst_4^{+/+}$) were then successfully bred on; animals used for the experiments were males strictly within the first 3 inbred generations. In the carrageenan- and endotoxin-evoked inflammation models $sst_4^{+/+}$ and $sst_4^{-/-}$ littermates were also tested for comparison. In the behavioral tests the experimenter was blind to the genotype.

Carrageenan-Induced Paw Inflammation Model. $Sst_4^{+/+}$ and $sst_4^{-/-}$ mice bred as separate lines were tested simultaneously with littermate controls in this model. Carrageenan (3%, 50 μL) was injected intraplantarly into the left hindpaw to induce subacute inflammation. The mechanonociceptive threshold of the paw was determined with dynamic plantar esthesiometry (Ugo Basile 37400) and the volume with plethysmometry (Ugo Basile 7140) before and 6 h after carrageenan injection. Separate groups of $sst_4^{+/+}$ and $sst_4^{-/-}$ littermates were pretreated with the selective sst_4 receptor agonist J-2156 (100 μg/kg i.p. 10 min before carrageenan). Data were expressed as percentage changes compared with the self-control values obtained before the induction of inflammation (20).

Adjuvant-Evoked Chronic Inflammation Model. Inflammation of the tibiotarsal joints was evoked by s.c. injection of complete CFA (killed *Mycobacteria* suspended in paraffin oil; 50 μL, 1 mg/mL) intraplantarly into the left hindpaw and the root of the tail. Paw volume was measured by plethysmometry, mechanical touch sensitivity by esthesiometry, and weight bearing with an incapacitance tester (Linton Instrumentation) before and 9 times after CFA administration during a 21-day period.

Endotoxin-Induced Airway Inflammation Model. Subacute pneumonitis was evoked by 60 μL *Escherichia coli* LPS (167 μg/mL dissolved in sterile PBS) applied intranasally 24 h before measurement (9, 21, 22).

Airway responsiveness was determined by whole-body plethysmography (Buxco Research Systems) both in conscious, spontaneously breathing animals (6) and anesthetized, tracheotomized, mechanically ventilated mice. In unrestrained animals the Penh, calculated as [(expiratory time/relaxation time) − 1]/(maximum expiratory flow/maximum inspiratory flow), was determined as an indicator of bronchoconstriction (9, 21, 22). In separate groups of $sst_4^{+/+}$ and $sst_4^{-/-}$ littermates RL (ΔcmH_2O * sec/mL) was directly measured. The muscarinic receptor agonist carbachol (carbamylcholine; 5.5, 11, and 22 mM, 50 μL per mouse for 50 sec) was nebulized to induce bronchoconstriction 24 h after LPS instillation. Mean Penh and RL of the 15-min measurement periods after each carbachol were expressed as percentage increases above baseline to evaluate airway function and to compare the changes of these 2 parameters (for details see *SI Text*). At the end of the study bronchoalveolar lavage was performed in 1 series of experiments, and the lungs were excised for further (histologic, cytokine, and myeloperoxidase) examinations in the other series of experiments.

Semiquantitative scoring of the inflammatory changes in the lung sections stained with hematoxylin and eosin or periodic acid-Schiff (to visualize mucus-producing goblet cells) was performed by an expert pathologist blind to the experimental design, on the basis of perivascular edema, perivascular/peribronchial acute inflammation, goblet cell hyperplasia/metaplasia of the bronchioles, and mononuclear cell infiltration into the alveolar spaces (9, 21,

22, 40). The composite inflammation scores (ranging from 0 to 10) were obtained by adding these values. MPO activity indicating the number of accumulated granulocytes and macrophages in the lung was determined by spectrophotometry (23).

In a separate series of experiments, the number of inflammatory cells (granulocytes, lymphocytes, and macrophages) in the BALF (21) was determined with a Partec CyFlow space flow cytometer. Differentiation was made on the basis of the size and granulation; cell numbers were calculated by FloMax software (Partec). The concentrations of 3 inflammatory cytokines—IL-1β, TNF-α, and IFN-γ—were measured with ELISA (BD Sciences and R&D Systems) from both the lung homogenates and BALF samples (all technical details are described in *SI Text*).

Oxazolone-Induced Allergic Contact Dermatitis Model (Delayed-Type Hypersensitivity Reaction). Animals were sensitized on 2 consecutive days by smearing 2% oxazolone dissolved in 96% ethanol (50–50 μL) on the shaved abdomen. Six days later oxazolone was applied on the right ears (15–15 μL on both surfaces) to elicit allergic contact dermatitis; the ethanol-treated left ears served as controls (23). Ear diameter was measured with an engineer's micrometer (Moore and Wright) with 0.1-mm accuracy, before and after oxazolone smearing. Data were expressed as percentage increase of ear thickness compared with the initial values. Light microscopic examination was performed on the histologic slides (6-μm cross-sections, hematoxylin and eosin staining). Inflammatory cytokines (IL-2, IL-4, IL-5, IFN-γ, and TNF-α) were determined by cytokine cytometric bead array (Becton Dickinson Biosciences), and IL-1β was measured with ELISA (for details see *SI Text*).

Statistical Analysis. Most results were expressed as means $\pm$ SEM of $n = 8$–10 mice in each group and evaluated by one-way ANOVA followed by Bonferroni's modified *t* test. Histologic scores were demonstrated as box plots and analyzed with Kruskal-Wallis test followed by Dunn's test. In all cases $P < 0.05$ was considered significant.

Ethics. Experimental procedures were carried out according to the 1998/XXVIII Act of the Hungarian Parliament on Animal Protection (243/1988), complied with the recommendations of the Helsinki Declaration, and were approved by the Ethics Committee on Animal Research of Pécs University (license no. BA02/2000–16-2006).

ACKNOWLEDGMENTS. The authors thank Anikó Perkecz for the histologic slides and Helga Rabovszky for the expert breeding of the animals. This work was sponsored by Hungarian Grants OTKA K73044, OTKA NK78059, RET-008/2005, ETT-06–284/2006, ETT-287/2006, and GVOP-3.2.1–2004-04–0420/3.0. Z.H. was supported by a Janos Bolyai Postdoctoral Fellowship.

1. Szolcsányi J, Helyes Z, Oroszi G, Németh J, Pintér E (1998) Release of somatostatin and its role in the mediation of the anti-inflammatory effect induced by antidromic stimulation of sensory fibres of rat sciatic nerve. *Br J Pharmacol* 123:936–942.
2. Szolcsányi J, Pintér E, Helyes Z, Oroszi G, Németh J (1998) Systemic anti-inflammatory effect induced by counter-irritation through a local release of somatostatin from nociceptors. *Br J Pharmacol* 125:916–922.
3. Szolcsányi J, Pintér E, Helyes Z (2004) Sensocrine function of capsaicin-sensitive nociceptors mediated by somatostatin regulates against inflammation and hyperalgesia. In *Hyperalgesia*: *Molecular Mechanisms and Clinical Implications,* eds Handwerker HO, Brune K (IASP Press, Seattle), pp 113–128.
4. Pintér E, Helyes Z, Szolcsányi J (2006) Inhibitory effect of somatostatin on inflammation and nociception. *Pharmacol Ther* 112:440–456.
5. Hokfelt T, et al. (1976) Immunohistochemical evidence for separate populations of somatostatin-containing and substance P-containing primary afferent neurons in the rat. *Neuroscience* 1:131–136.
6. Lawson SN (1995) Neuropeptides in morphologically and functionally identified primary afferent neurons in dorsal root ganglia: Substance P, CGRP and somatostatin. *Prog Brain Res* 104:161–173.
7. Dux M, et al. (1999) Changes in fibre populations of the rat hairy skin following selective chemodenervation by capsaicin. *Cell Tissue Res* 296:471–477.
8. Helyes Z, et al. (2004) Antiinflammatory and analgesic effects of somatostatin released from capsaicin-sensitive sensory nerve terminals in a Freund's adjuvant-induced chronic arthritis model in the rat. *Arthritis Rheum* 50:1677–1685.
9. Helyes Z, et al. (2007) Role of transient receptor potential vanilloid 1 receptors in endotoxin-induced airway inflammation in the mouse. *Am J Physiol Lung Cell Mol Physiol* 292:L1173–L1181.
10. Patel YC, et al. (1995) The somatostatin receptor family. *Life Sci* 57:1249–1265.
11. ten Bokum AM, Hofland LJ, van Hagen PM (2000) Somatostatin and somatostatin receptors in the immune system: A review. *Eur Cytokine Netw* 11:161–176.
12. Maggi CA (1995) Tachykinins and calcitonin gene-related peptide (CGRP) as cotransmitters released from peripheral endings of sensory nerves. *Prog Neurobiol* 45:1–98.
13. van Hagen PM, et al. (1994) Somatostatin and the immune and haematopoetic system: A review. *Eur J Clin Invest* 24:91–99.
14. Hoyer D, et al. (1995) Classification and nomenclature of somatostatin receptors. *Trends Pharmacol Sci* 16:86–88.
15. Helyes Z, et al. (2001) Anti-inflammatory effect of synthetic somatostatin analogues in the rat. *Br J Pharmacol* 134:1571–1579.
16. Pintér E, et al. (2002) Pharmacological characterisation of the somatostatin analogue TT-232: Effects on neurogenic and non-neurogenic inflammation and neuropathic hyperalgesia. *Naunyn Schmiedebergs Arch Pharmacol* 366:142–150.
17. Allen JP, et al. (2003) Somatostatin receptor 2 knockout/lacZ knockin mice show impaired motor coordination and reveal sites of somatostatin action within the striatum. *Eur J Neurosci* 17:1881–1895.
18. Schwenk F, Baron U, Rajewsky K (1995) A cre-transgenic mouse strain for the ubiquitous deletion of loxP-flanked gene segments including deletion in germ cells. *Nucleic Acids Res* 23:5080–5081.
19. Helyes Z, et al. (2006) Effects of the somatostatin receptor subtype 4 selective agonist J-2156 on sensory neuropeptide release and inflammatory reactions in rodents. *Br J Pharmacol* 149:405–415.
20. Sándor K, et al. (2006) Analgesic effects of the somatostatin sst_4 receptor selective agonist J-2156 in acute and chronic pain models. *Eur J Pharmacol* 539:71–75.
21. Elekes K, et al. (2008) Inhibitory effects of synthetic somatostatin receptor subtype 4 agonists on acute and chronic airway inflammation and hyperreactivity in the mouse. *Eur J Pharmacol* 578:313–322.
22. Elekes K, et al. (2007) Role of capsaicin-sensitive afferents and sensory neuropeptides in endotoxin-induced airway inflammation and consequent bronchial hyperreactivity in the mouse. *Regul Pept* 141:44–54.
23. Bánvölgyi Á, et al. (2005) Evidence for a novel protective role of the vanilloid TRPV1 receptor in a cutaneous contact allergic dermatitis model. *J Neuroimmunol* 169:86–96.
24. Pintér E, Szolcsányi J (1996) Systemic anti-inflammatory effect induced by antidromic stimulation of the dorsal roots in the rat. *Neurosci Lett* 212:33–36.
25. Szabó Á, et al. (2008) Investigation of sensory neurogenic components in a bleomycin-induced scleroderma model using transient receptor potential vanilloid 1 receptor- and calcitonin gene-related peptide-knockout mice. *Arthritis Rheum* 58:292–301.
26. Elliott DE, et al. (1999) SSTR2A is the dominant somatostatin receptor subtype expressed by inflammatory cells, is widely expressed and directly regulates T cell IFN-gamma release. *Eur J Immunol* 29:2454–2463.
27. Muscettola M, Grasso G (1990) Somatostatin and vasoactive intestinal peptide reduce interferon gamma production by human peripheral blood mononuclear cells. *Immunobiology* 180:419–430.
28. Berman AS, Chancellor-Freeland C, Zhu G, Black PH (1996) Substance P primes murine peritoneal macrophages for an augmented proinflammatory cytokine response to lipopolysaccharide. *Neuroimmunomodulation* 3:141–149.
29. Niedermuhlbichler M, Wiedermann CJ (1992) Suppression of superoxide release from human monocytes by somatostatin-related peptides. *Regul Pept* 41:39–47.
30. Chowers Y, et al. (2000) Somatostatin through its specific receptor inhibits spontaneous and TNF-alpha- and bacteria-induced IL-8 and IL-1 beta secretion from intestinal epithelial cells. *J Immunol* 165:2955–2961.
31. Sener G, Cetinel S, Erkanli G, Gedik N, Yegen BC (2005) Octreotide ameliorates sepsis-induced pelvic inflammation in female rats by a neutrophil-dependent mechanism. *Peptides* 26:493–499.
32. Partsch G, Matucci-Cerinic M (1992) Effect of substance P and somatostatin on migration of polymorphonuclear (PMN) cells in vitro. *Inflammation* 16:539–547.
33. Kolasinski SL, Haines KA, Siegel EL, Cronstein BN, Abramson SB (1992) Neuropeptides and inflammation. A somatostatin analog as a selective antagonist of neutrophil activation by substance P. *Arthritis Rheum* 35:369–375.
34. Torrecillas G, Medina J, Diez-Marques ML, Rodriguez-Puyol D, Rodriguez-Puyol M (1999) Mechanisms involved in the somatostatin-induced contraction of vascular smooth muscle cells. *Peptides* 20:929–935.
35. Tigerstedt NM, Aavik E, Aavik S, Savolainen-Peltonen S, Hayry P (2007) Vasculoprotective effects of somatostatin receptor subtypes. *Mol Cell Endocrinol* 279:34–38.
36. ten Bokum AM, et al. (1999) Somatostatin receptor subtype expression in cells of the rat immune system during adjuvant arthritis. *J Endocrinol* 161:167–175.
37. Taniyama Y, et al. (2005) Systemic distribution of somatostatin receptor subtypes in human: An immunohistochemical study. *Endocr J* 52:605–611.
38. Gulya K, et al. (1986) Cyclic somatostatin octapeptide analogues with high affinity and selectivity toward mu opioid receptors. *Life Sci* 38:2221–2229.
39. Vásquez C, Lewis DL (1999) The CB1 cannabinoid receptor can sequester G-proteins, making them unavailable to couple to other receptors. *J Neurosci* 19:9271–9280.
40. Zeldin DC, et al. (2001) Airway inflammation and responsiveness in prostaglandin H synthase-deficient mice exposed to bacterial lipopolysaccharide. *Am J Respir cell Mol Biol* 25:457–465.